NASA Technical Memorandum 84545

Application of Zimmerman Flutter-Margin Criterion to a Wind-Tunnel Model

Robert M. Bennett

NOVEMBER 1982

NASA

NASA Technical Memorandum 84545

Application of Zimmerman Flutter-Margin Criterion to a Wind-Tunnel Model

Robert M. Bennett
Langley Research Center
Hampton, Virginia

National Aeronautics
and Space Administration

Scientific and Technical Information Branch

1982

SUMMARY

A brief study of the Zimmerman flutter-margin criterion has been made by applying it to data obtained from a wind-tunnel model. The sensitivity of the flutter-margin parameter was explored with a parametric trend study and by calculation of the derivatives with respect to the input frequency and damping parameters. The criterion is simple in concept and application, and it serves as a good flutter-onset predictor because it gives a nearly linear variation with dynamic pressure. However, accurate values of both frequency and damping of both modes involved in flutter are required for reliable flutter-onset prediction. The simplified version using only frequencies gave a highly nonconservative flutter onset in one case and should not be used in general. Normalizing the flutter-margin parameter by the wind-off values of the simplified flutter-margin parameter yields a parameter of the order of 1.0 to 0, and this is the recommended procedure.

INTRODUCTION

One difficult aspect of flutter testing is that a flutter mode can suddenly become unstable with only a small increase in dynamic pressure. Furthermore, there may be little or no indication of the approach of the instability in a plot of modal damping against dynamic pressure. Although such a sudden onset of instability is not always the case, it occurs in practice frequently enough that flutter prediction based on the projection of modal damping may not be adequate. The development of techniques for determining the nearness of flutter onset has received considerable attention. (See refs. 1 to 8, for example.) These flutter-prediction techniques, which vary considerably in form and complexity, extend from projections of inverse peak amplitude of modal response to ambient excitation (ref. 7, for example) to projections based on the differential equations of motion using coefficients determined from the dynamic measurements of forced response (ref. 3). The technique to be used in practice depends on such factors as the availability of input forcing, instrumentation, the amount of computation and analysis required, and whether an on-line or off-line technique is required. In many cases, no single technique is sufficient and the use of several techniques is required for reliable flutter-onset prediction. The purpose of this paper is to present the results of a brief study of one technique that was previously developed (ref. 2) and that is commonly referred to as the Zimmerman flutter criterion.

The Zimmerman flutter criterion is based on considering the value of Routh's discriminant for the characteristic equation of a two-degree-of-freedom system as a flutter-margin parameter. It can be expressed in terms of the measured frequency and damping of the two modes which are input as parameters. Although this technique was developed over 15 years ago, it has not been widely used because it requires measured values of the frequencies and dampings of both modes involved in the flutter condition. Typically, the damping of one of the modes increases so rapidly as flutter is approached that it becomes difficult to measure and is, thus, unavailable. With modern testing and data-analysis techniques, this difficulty should be alleviated and the criterion should be of more interest than in the past.

The flutter-margin criterion and its analytical development are described in this report. The criterion is applied to a wind-tunnel flutter model for which some analytical and experimental data are available. (See ref. 9.) The sensitivity of the flutter margin to the modal frequencies and dampings is evaluated with a parametric trend study and with the development of derivatives of the flutter-margin parameter.

SYMBOLS

A_j	coefficients of characteristic equations, where $j = 0,1,2,3$
c	chord
F	flutter-margin parameter normalized by simplified value of $\tilde{F}_{s,0}$
$\tilde{F}$	flutter-margin parameter
F_s	simplified flutter-margin parameter normalized by $\tilde{F}_{s,0}$
$\tilde{F}_s$	simplified flutter-margin parameter
$\tilde{F}_{s,0}$	simplified flutter-margin parameter evaluated at $q = 0$
f	frequency, $\omega/2\pi$, Hz
i	$= \sqrt{-1}$
M	free-stream Mach number
q	free-stream dynamic pressure, psf
β	real part of complex characteristic root (decay rate or damping), 1/sec
λ	complex characteristic root, $\beta + i\omega$
ω	imaginary part of complex characteristic root (frequency), rad/sec

Subscript:

i	modal index, $i = 1,2$

ANALYSIS

Zimmerman Flutter-Margin Criterion

The stability of a two-degree-of-freedom flutter system with quasi-static aerodynamics is given by the quartic characteristic equation

$$\lambda^4 + A_3\lambda^3 + A_2\lambda^2 + A_1\lambda + A_0 = 0 \qquad (1)$$

where the values of A are real. The roots λ are usually two complex pairs

$$\lambda_{1,2} = \beta_1 \mp i\omega_1$$

$$\lambda_{3,4} = \beta_2 \mp i\omega_2$$

The boundary for neutral stability is given by Routh's criterion

$$A_2\left(\frac{A_1}{A_3}\right) - \left(\frac{A_1}{A_3}\right)^2 - A_0 = 0 \tag{2}$$

For a stable condition, this equation is not satisfied and the left-hand side of equation (2) yields a positive number $\tilde{F}$, which is defined as the Zimmerman flutter-margin parameter and is generally called the Zimmerman flutter criterion. The values of A can be expressed in terms of β and ω by expanding the factored equation

$$(\lambda - \beta_1 + i\omega_1)(\lambda - \beta_1 - i\omega_1)(\lambda - \beta_2 + i\omega_2)(\lambda - \beta_2 - i\omega_2) = 0 \tag{3}$$

and comparing the terms with those of equation (1). Then, F can be expressed in terms of β and ω as follows:

$$\tilde{F} = \left[1 - \left(\frac{\beta_2 - \beta_1}{\beta_2 + \beta_1}\right)^2\right]\left\{\left(\frac{{\omega_2}^2 - {\omega_1}^2}{2}\right)^2 + (\beta_1 + \beta_2)^2\left[\left(\frac{{\omega_2}^2 + {\omega_1}^2}{2}\right) + \left(\frac{\beta_1 + \beta_2}{2}\right)^2\right]\right\} \tag{4}$$

Note that

$$1 - \left(\frac{\beta_2 - \beta_1}{\beta_2 + \beta_1}\right)^2 = 0$$

if either β_1 or $\beta_2 = 0$ and, consequently, $\tilde{F} = 0$. Equation (4) is one of the many algebraic forms of the Zimmerman criterion (eq. (A21) of ref. 2) that can be obtained by manipulation of equation (A20) of reference 2.

A simplified version of equation (4) can be derived by using only static aerodynamics, where all modes are undamped up to the speed for frequency coalescence. Letting $\beta_1 = \beta_2 \to 0$ in equation (4) gives the result

$$\tilde{F}_s = \left(\frac{\omega_2^2 - \omega_1^2}{2}\right)^2$$

where the subscript s denotes the static aerodynamic value.

The values calculated for $\tilde{F}$ in equation (4) tend to be large and of the order of ω_2^4. A convenient way of normalizing $\tilde{F}$ is by substituting the value of F_s at $q = 0$. Thus, by letting

$$\tilde{F}_{s,0} = \left(\frac{\omega_2^2 - \omega_1^2}{2}\right)^2_{q=0}$$

and

$$F = \tilde{F}/\tilde{F}_{s,0}$$

the result is

$$F = \frac{1}{\tilde{F}_{s,0}}\left[1 - \left(\frac{\beta_2 - \beta_1}{\beta_2 + \beta_1}\right)^2\right]\left\{\left(\frac{\omega_2^2 - \omega_1^2}{2}\right)^2 + (\beta_1 + \beta_2)^2\left[\left(\frac{\omega_2^2 + \omega_1^2}{2}\right) + \left(\frac{\beta_1 + \beta_2}{2}\right)^2\right]\right\} \tag{5}$$

which gives a parameter that is normally in the range from 1.0 to 0. Normalizing F_s in the same manner gives

$$F_s = \frac{1}{\tilde{F}_{s,0}}\left(\frac{\omega_2^2 - \omega_1^2}{2}\right)^2 \tag{6}$$

Note that F_s is always positive and is zero only when $\omega_2 = \omega_1$.

For flutter-onset prediction, F is calculated from measured values of β and ω for several discrete values of dynamic pressure at constant Mach number. A least-squares fit of a straight line can then be used to project to flutter onset (where $F = 0$). The fit and the onset prediction can be updated as further points are measured.

It can be shown that for quasi-static aerodynamics and without structural damping, F is a quadratic equation with dynamic pressure q. (See ref. 2.) Use can be made of the quadratic relation in order to project to flutter. However, with unsteady aerodynamics the relation is more complex than quadratic and, thus, this relation is not used herein. If aerodynamic lags of higher order than quasi-static are considered (such as exponential lags for the indicial response), the quartic equation (1) becomes a polynomial of higher degree.

Derivatives of F

The sensitivity of F to all the input values of β_1 can be determined by differentiating equation (5) and calculating $dF/d\beta_1$. The resulting equations are

$$\frac{dF}{d\omega_1} = 4\beta_1\beta_2\omega_1\left[1 - \frac{\omega_2^2 - \omega_1^2}{(\beta_1 + \beta_2)^2}\right]\Bigg/\tilde{F}_{s,0} \tag{7a}$$

$$\frac{dF}{d\omega_2} = 4\beta_1\beta_2\omega_2\left[1 + \frac{\omega_2^2 - \omega_1^2}{(\beta_1 + \beta_2)^2}\right]\Bigg/\tilde{F}_{s,0} \tag{7b}$$

$$\frac{dF}{d\beta_1} = \beta_2\left[2\beta_1(\beta_1 + \beta_2) + W\right]\Big/\tilde{F}_{s,0} \tag{7c}$$

$$\frac{dF}{d\beta_2} = \beta_1\left[2\beta_2(\beta_1 + \beta_2) + W\right]\Big/\tilde{F}_{s,0} \tag{7d}$$

where

$$W = (\beta_1 + \beta_2)^2 + 2\left(\omega_1^2 + \omega_2^2\right) + \frac{\beta_2 - \beta_1}{(\beta_1 + \beta_2)^3}\left(\omega_2^2 - \omega_1^2\right)^2 \tag{8}$$

The derivatives $dF/d\omega_1$ and $dF/d\omega_2$ are evaluated, respectively, in terms of f_1 and f_2, in hertz, by

$$\frac{dF}{df_1} = 2\pi \frac{dF}{d\omega_1} \tag{9a}$$

$$\frac{dF}{df_2} = 2\pi \frac{dF}{d\omega_2} \tag{9b}$$

Similar results for F_s are as follows:

$$\frac{dF_s}{d\omega_1} = -\omega_1\left(\omega_2^{\,2} - \omega_1^{\,2}\right)\Big/\tilde{F}_{s,0} \tag{10a}$$

$$\frac{dF_s}{d\omega_2} = \omega_2\left(\omega_2^{\,2} - \omega_1^{\,2}\right)\Big/\tilde{F}_{s,0} \tag{10b}$$

Alternative derivatives with respect to ω^2 may be more appropriate since F_s depends only on the squares of ω_1 and ω_2 and are, respectively,

$$\frac{dF_s}{d\omega_1^{\,2}} = -\frac{1}{2}\left(\omega_2^{\,2} - \omega_1^{\,2}\right)\Big/\tilde{F}_{s,0} \tag{11a}$$

$$\frac{dF_s}{d\omega_2^{\,2}} = \frac{1}{2}\left(\omega_2^{\,2} - \omega_1^{\,2}\right)\Big/\tilde{F}_{s,0} \tag{11b}$$

RESULTS AND DISCUSSION

Description of Model and Tests

The sample case used for application of the flutter-margin criterion is the wind-tunnel model of references 9 and 10. The planform is shown in figure 1. The wing was of conventional flutter-model construction with a spar and pods and was cantilevered from a sidewall mount. It was flutter tested in the Langley Transonic Dynamics Tunnel by varying the test-medium density (Freon[1]) at a constant Mach number for Mach numbers of 0.6 and 0.9. Experimental flutter points are given in refer-

---

[1]Freon: Registered trademark of E. I. du Pont de Nemours & Co., Inc.

ences 9 and 10. Calculations for subcritical values of density at $M = 0.6$ and 0.9 are given in reference 9 and are used herein. The subcritical calculations are based on fitting doublet lattice aerodynamic forces for harmonic motion with a ratio of polynomials in reduced frequency, and then on using the fitted function to generalize for transient motions. (See refs. 9 and 10.) In addition, some limited, previously unpublished, experimental data at subcritical densities were available. The frequencies of the first two modes were determined from on-line spectral measurements of accelerometer response to wind-tunnel turbulence. Ensemble-averaged spectra in the range from 0 to 50 Hz were taken by using 20 ensemble averages (102 sec of data). The frequencies of the first two modes were determined from the peaks. Damping and frequency values for the first mode were also determined from fast frequency sweeps of the control surface (from 2 to 20 Hz in 20 sec) for subcritical conditions at $M = 0.9$. The records were analyzed by using the methods and equipment described in reference 11. No information on the damping of the second mode was available. The flutter data (refs. 9 and 10) indicate that the bottom of the transonic dip is above $M = 0.9$. The first two mode frequencies calculated by a finite-element method (ref. 9) are 5.23 Hz and 19.13 Hz. The corresponding measured values are 5.2 Hz and 19.2 Hz. The first mode is first wing bending, and the second mode is a combined bending and torsion mode. Although references 9 and 10 describe active flutter-suppression tests, only the data for the wing with the flutter-suppression system off are considered herein.

Flutter-Margin Calculations

The calculated frequencies and decay rates for the first two modes (from ref. 9) and the corresponding values of F and F_s are shown in figures 2 and 3 for Mach numbers of 0.6 and 0.9, respectively. The corresponding experimental flutter points (figs. 2 and 3) are in good agreement with the calculated values. For both Mach numbers, the variation of F with q produces nearly a straight line, except near $q = 0$, and, thus, would serve as a much better projector to flutter than modal decay rate or damping. For example, for $M = 0.6$, damping of the flutter mode changes curvature and slope and then becomes unstable between $q = 130$ and 155 psf, whereas F is nearly a straight line for $q \geqslant 80$ psf. It might also be noted that the calculated frequency and damping values are based on solutions using 10 calculated vibration modes and unsteady aerodynamics. The influence of the vibration modes above the second mode on the calculated values of F is apparently small in this case.

For $M = 0.6$ (fig. 2(c)), F_s is quite close to F, except near $q = 0$. For this case, the modal frequencies are, in fact, near coalescence at flutter. However, F_s does not go to zero but remains a small positive number since the modal frequencies are not equal at flutter as assumed for F_s. For $M = 0.9$ (fig. 3(c)), F_s is not close to F because the modal frequencies are not near coalescence, even at flutter. The use of F_s as a predictor would overestimate the flutter dynamic pressure by 30 percent. This unconservative estimate indicates that, in general, F_s should not be used for flutter-onset prediction.

Derivatives of Flutter-Margin Parameter

The derivatives of F with respect to the input parameters β_1, β_2, f_1, and f_2 are presented in figures 4 and 5. These derivatives are calculated from equations (7) to (9) for the two Mach numbers and the dynamic pressures of the sample case by using the frequency and damping (decay-rate) values from figures 2 and 3. These derivatives indicate the local sensitivity of F to small changes in the input parameters (such as measurement error) and indicate the emphasis that should be given to each measurement. An extreme sensitivity would indicate a difficulty with the method.

At the flutter point, all the derivatives, except $dF/d\beta_1$, are zero because β_1 is zero. Thus, β_1 is the only significant parameter near flutter for this case where flutter occurs in the first mode. As previously indicated in the "Analysis" section, $F = 0$ if either β_1 or $\beta_2 = 0$; thus, the low damping of the flutter mode determines F at or near the flutter point. The primary concern, however, is not at the flutter point but with the sensitivity of F at subcritical speeds for use in projecting to flutter. The derivatives of $dF/d\beta_1$ and $dF/d\beta_2$ are very large near $q = 0$ where both β_1 and β_2 are small (essentially structural damping). This result indicates that the large differences in F and F_s near $q = 0$ (figs. 2 and 3) result from the inclusion of damping in F. For this case, the derivatives $dF/d\beta_1$ and $dF/d\beta_2$ are large where the frequencies of the two modes are well separated, and they are small when the frequencies are near coalescence. If a measurement error of 1.0 rad/sec is assumed for β_1, the change in F for $60 \text{ psf} < q < 100 \text{ psf}$ would be relatively small for $M = 0.6$ (fig. 4), but it would be of the order of 0.1 to 0.2 for $M = 0.9$. Although $dF/d\beta_2$ is smaller than $dF/d\beta_1$, the measurement error would be expected to be correspondingly larger where β_2 is large and its measurement more difficult. Thus, F would also be significantly influenced by β_2 away from the flutter point.

The derivative dF/df_2 is generally much larger than the derivative dF/df_1 (figs. 4 and 5) and differs in sign; this indicates that F is more sensitive to f_2 than f_1. The derivatives of F_s, the simplified criterion which is given by equation (10), indicate that dF_s/df_2 should be larger than dF_s/df_1 by the ratio of the two frequencies and it should be of opposite sign. Similar results for F are apparent in figures 4 and 5. The value of dF/df_1 is nearly a constant at small values of q and is small when considering a reasonable measurement error for f_1 of 0.25 Hz. The value of dF/df_2 is larger at small values of q where the frequencies are well separated, and it decreases to become of nearly the same order of magnitude as dF/df_1 as the two frequencies approach the flutter condition.

Overall, the sensitivities indicated by figures 4 and 5 are reasonable; and any scatter in F would be expected to be of the order of magnitude of any scatter in β and ω, except for the damping parameters near $q = 0$.

Parametric Trend Study

The expression for F (eq. (5)) is a simple algebraic function of the four parameters β_1, β_2, ω_1, and ω_2. The influence of each parameter can be evaluated by varying each parameter with the other three held constant. The results, which are presented in figure 6, complement the local sensitivities given by the derivatives discussed in the previous section by indicating the change in F for finite changes in the parameters.

The variation of F with β_1 for several values of β_2 is shown in figure 6(a) for values of frequency at $q = 0$. The frequencies for this case are well separated and, as previously indicated, F is very sensitive to β_1 for small initial values of β_1 or β_2. Moderate sensitivity is still indicated (by the slope of the curves) for moderate values of both β_1 and β_2, and less sensitivity is indicated for large values of either β_1 or β_2. Similar trends are noted for varying β_2 for constant values of β_1. (See fig. 6(b).)

The variation of F with f_1 for constant values of f_2 is shown in figure 6(c), and the variation of F with f_2 for constant values of f_1 is shown in figure 6(d). For these cases, F is normalized by $\tilde{F}_{s,0}$ with $f_1 = 5.23$ Hz and $f_2 = 19.13$ Hz. The value of F, therefore, varies considerably as f_1 and f_2 are varied. For this case with small values of β_1 and β_2, F is sensitive to f_1 only when f_1 approaches f_2 (fig. 6(c)), where F becomes nearly zero. Similar trends are noted as f_2 is varied (fig. 6(d)), but there is considerable sensitivity to f_2 (large slope) for larger values of f_2 as previously indicated by the derivatives.

Calculations Using Limited Experimental Data

A limited amount of subcritical frequency and damping data for the first two modes were available from the experiment. In this section, flutter-onset prediction is examined by using a combination of the available experimental data and the analytical results.

The frequencies of the first two modes from ensemble-averaged spectral measurements are compared in figure 7 with the calculated values from figures 2 and 3. There is good overall agreement, although there are some differences in the values of the first-mode frequency, and there is some scatter in the measured frequencies for the second mode. The corresponding values of F calculated by using the measured frequencies and the calculated damping values (from figs. 2 and 3) are shown in figure 8. The use of the measured frequencies results in little change in F except for the lower dynamic pressures. As previously indicated, $F \to 0$ as $\beta_1 \to 0$ and β_1 determines the value of F near the flutter point. The measured frequencies, thus, have little influence near the flutter point. At the lower values of dynamic pressure, using the measured frequencies for this case would lead to an underprediction of the flutter point. Thus, using the measured frequencies does not significantly improve flutter-onset prediction.

The values of frequency and damping of the first mode as determined from fast frequency sweeps are compared in figure 9 with the calculated values from figure 3 for $M = 0.9$. The measured frequencies are in good agreement with those from the ensemble-averaged spectral measurements. (Compare figs. 7 and 9.) The measured damping values show the same trend as the calculations and are in good agreement with the calculated values at low dynamic pressures. They differ near the flutter point because the calculations predict a somewhat lower dynamic pressure at flutter. The corresponding values of F calculated by using the measured results for the first mode and the calculated results for the second mode are presented in figure 10. They are also compared with the results obtained from using calculated values of both the first and second modes. The experimental flutter point is closely defined by the values of F (fig. 10), whereas the measured values of β_1 do not define the experimental flutter point nearly as well (fig. 9). Flutter-onset prediction from the values of F for $q < 80$ psf would be impossible, however, as a result of the scatter in the measured values. (See fig. 10.)

It appears that reliable onset prediction requires accurate measurement of the frequency and damping of both modes. Although mixing some calculated and measured results was helpful in one case, the general use of this technique is questionable.

General Comments on the Technique

One of the factors discussed in the previous sections is the sensitivity of the results to the input damping and frequencies. Overall, the sensitivity was reasonable and the scatter in F would be of the same order as that in the individual damping and frequency values used to compute F. However, the plot of F against q is nearly linear and would, thus, be less sensitive to scatter than would the complex curves that are obtained by plotting damping against q. Some improvement may also be gained by considering projections based on a quadratic function for F plotted against q as can be seen in figure 2(c), where F plotted against q is somewhat nonlinear. It is preferable to use linear extrapolations wherever possible and to limit nonlinear projections to a very small range of projection. Thus, caution should be exercised if the quadratic projection is used.

The brief results of this report have also indicated that further emphasis should be given to the accurate measurement of the frequency and damping of the second mode in addition to the flutter mode. In general, this is a difficult task and may require special excitation techniques when the damping of the second mode is large.

The application cited here and the development of the criterion presented herein have considered the case of flutter involving only two aeroelastic modes. It might be noted, however, that at least one case has been reported in the literature (ref. 4) where the projection near flutter was quite nonlinear, possibly as a result of the involvement of more than two modes in the flutter condition. The equivalent Routh's discriminant can be readily derived for more than two modes, but its application to flutter data has not yet been reported. In addition, other methods have recently been developed (ref. 8) that may complement the use of the Zimmerman criterion for multimodal situations.

The result of the application of the Zimmerman criterion to wind-tunnel and flight flutter testing is apparent. Other applications may be for the projection to flutter from the output of time-dependent, transonic, aeroelastic analysis codes, such as that of reference 12.

CONCLUSIONS

A brief study of the Zimmerman flutter-margin criterion has been made by applying it to data obtained from a wind-tunnel model. The sensitivity of the flutter-margin parameter was explored with a parametric trend study and by calculation of the derivatives with respect to the input frequency and damping parameters. The results of this investigation indicate the following conclusions:

1. The criterion is simple in concept and application, and it serves as a good flutter-onset predictor because it gives a nearly linear variation with dynamic pressure.

2. Emphasis should be given to the accurate measurement of the frequency and damping of both modes involved in the flutter condition for reliable flutter-onset prediction.

3. The simplified version using only frequencies predicted a highly nonconservative flutter onset for one case and, thus, should not be used in general.

4. Normalizing the flutter-margin parameter by the wind-off values of the simplified flutter-margin parameter yields a parameter of the order of 1.0 to 0, and this is the recommended procedure.

Langley Research Center
National Aeronautics and Space Administration
Hampton, VA 23665
September 28, 1982

REFERENCES

1. Flutter Testing Techniques. NASA SP-415, 1976.

2. Zimmerman, Norman H.; and Weissenburger, Jason T.: Prediction of Flutter Onset Speed Based on Flight Testing at Subcritical Speeds. J. Aircr., vol. 1, no. 4, July-Aug. 1964, pp. 190-202.

3. Heron, K. H.; Gaukroger, D. R.; and Skingle, C. W.: The Derivation of Equations of Motion From Response Data, and Its Application in Flutter Testing. Tech. Rep. 73051, British R.A.E., June 1973.

4. Skingle, C. W.; and Gaukroger, D. R.: An Application of Fast Frequency-Sweep Excitation to the Measurement of Sub-Critical Response of a Low Speed Wind Tunnel Model. C.P. No. 1356, British A.R.C., 1976.

5. Copley, J. C.: Numerical Analysis of Vector Responses. Tech. Rep. 80135, British R.A.E., Nov. 1980.

6. Bennett, Robert M.; and Abel, Irving: Flight Flutter Test and Data Analysis Techniques Applied to a Drone Aircraft. J. Aircr., vol. 19, no. 7, July 1982, pp. 589-595.

7. Ruhlin, Charles L.; Watson, Judith J.; Ricketts, Rodney H.; and Doggett, Robert V., Jr.: Evaluation of Four Subcritical Response Methods for On-Line Prediction of Flutter Onset in Wind-Tunnel Tests. A Collection of Technical Papers, Part 2: Structural Dynamics and Design Engineering - AIAA/ASME/ASCE/AHS 23rd Structures, Structural Dynamics and Materials Conference, May 1982, pp. 94-101. (Available as AIAA-82-0644.)

8. Matsuzaki, Yuji; and Ando, Yasukatsu: Estimation of Flutter Boundary From Random Responses Due to Turbulence at Subcritical Speeds. J. Aircr., vol. 18, no. 10, Oct. 1981, pp. 862-868. (Available as AIAA-81-4267.)

9. Abel, Irving: An Analytical Technique for Predicting the Characteristics of a Flexible Wing Equipped With an Active Flutter-Suppression System and Comparison With Wind Tunnel Data. NASA TP-1367, 1979.

10. Newsom, Jerry R.; Abel, Irving; and Dunn, H. J.: Application of Two Design Methods for Active Flutter Suppression and Wind-Tunnel Test Results. NASA TP-1653, 1980.

11. Edwards, John W.: Flight Test Results of an Active Flutter Suppression System Installed on a Remotely Piloted Research Vehicle. A Collection of Technical Papers, Part 2 - AIAA/ASME/ASCE/AHS 22nd Structures, Structural Dynamics and Materials Conference and AIAA Dynamics Specialists Conference, Apr. 1981, pp. 778-789. (Available as AIAA-81-0655.)

12. Borland, C. J.; and Rizzetta, D. P.: Nonlinear Transonic Flutter Analysis. AIAA-81-0608-CP, Apr. 1981.

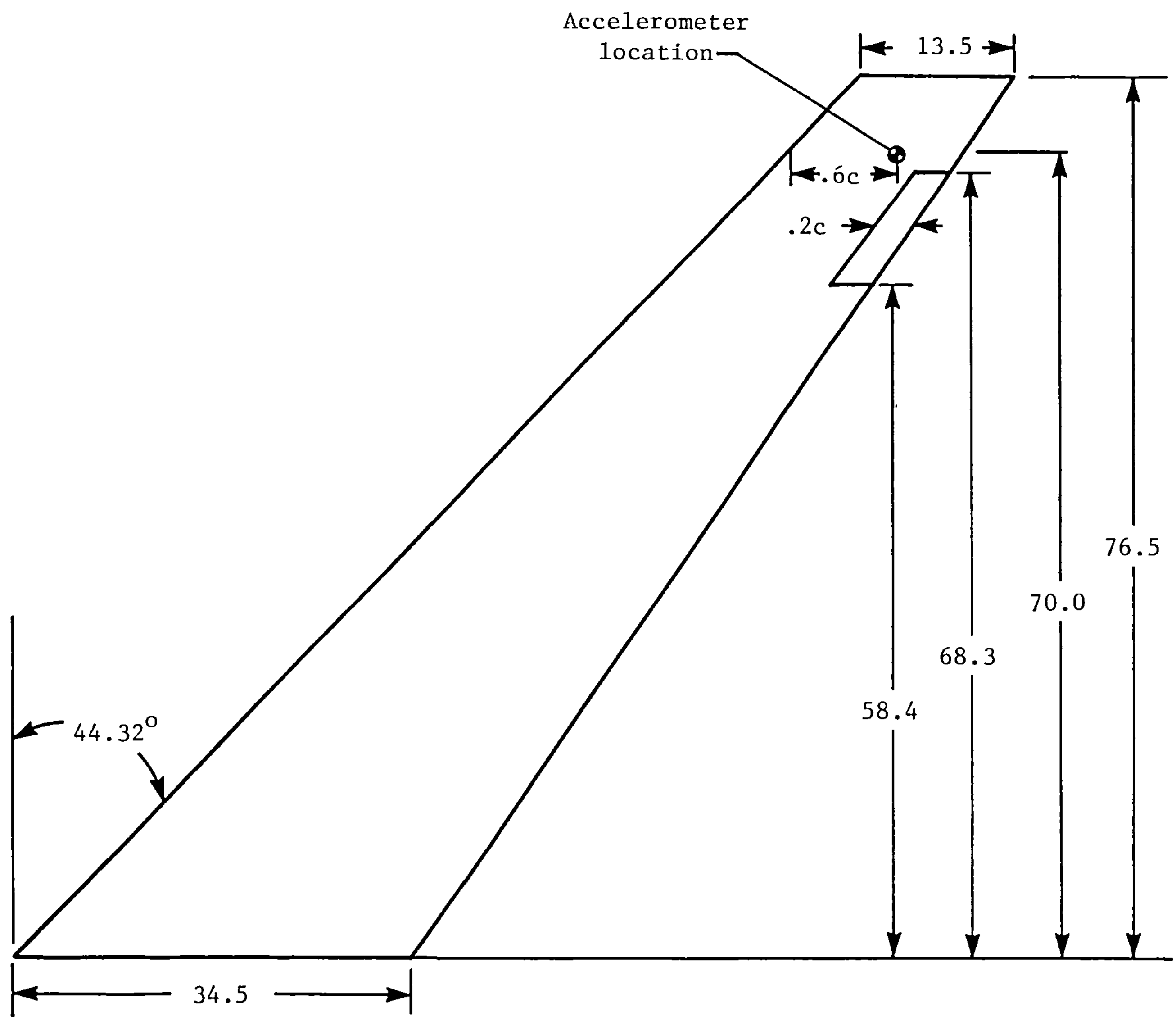

Figure 1.- Geometry of wind-tunnel model. All dimensions are given in inches unless otherwise specified.

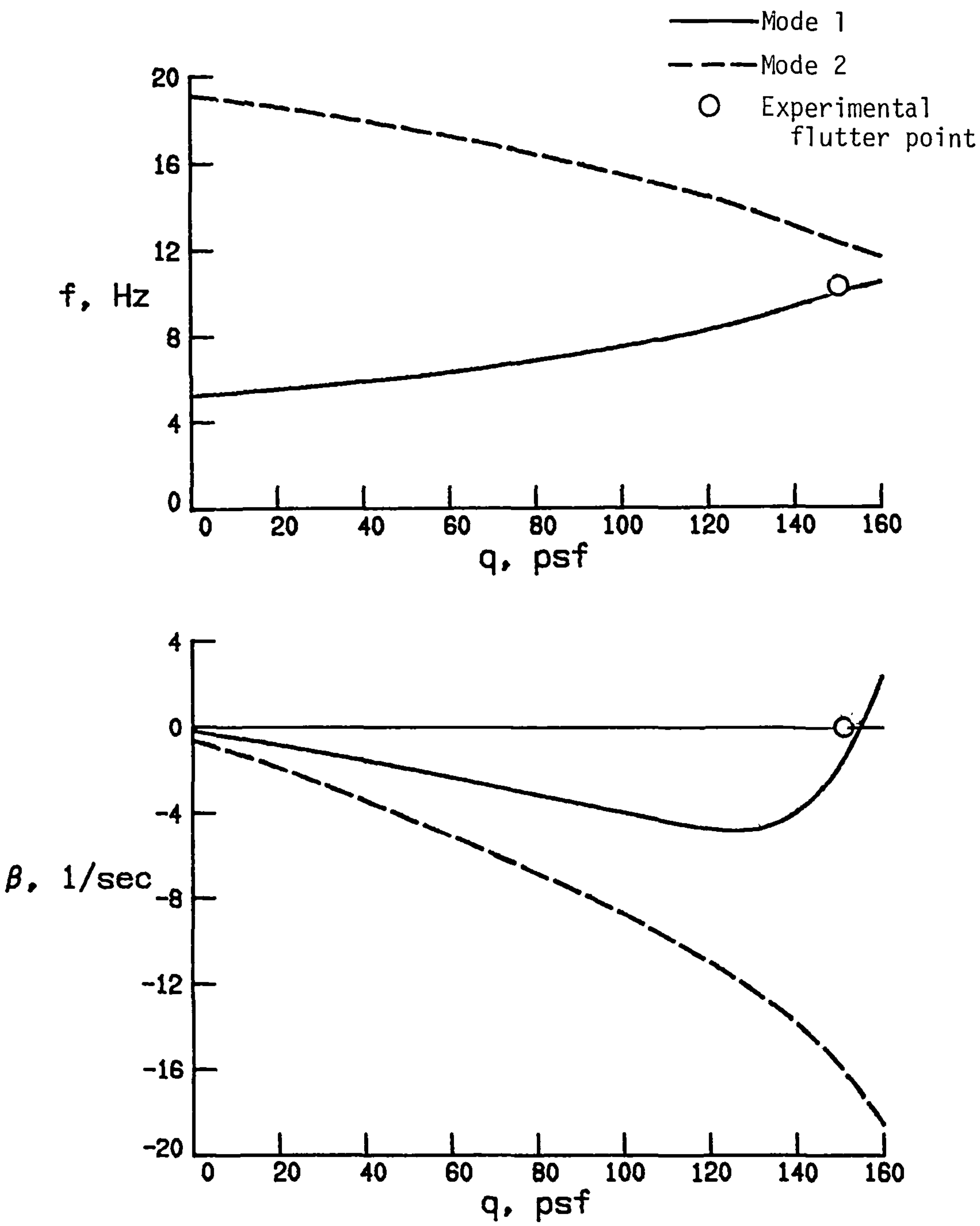

(a) Frequencies and decay rates.

Figure 2.- Calculated dynamic characteristics for wind-tunnel model for $M = 0.6$.

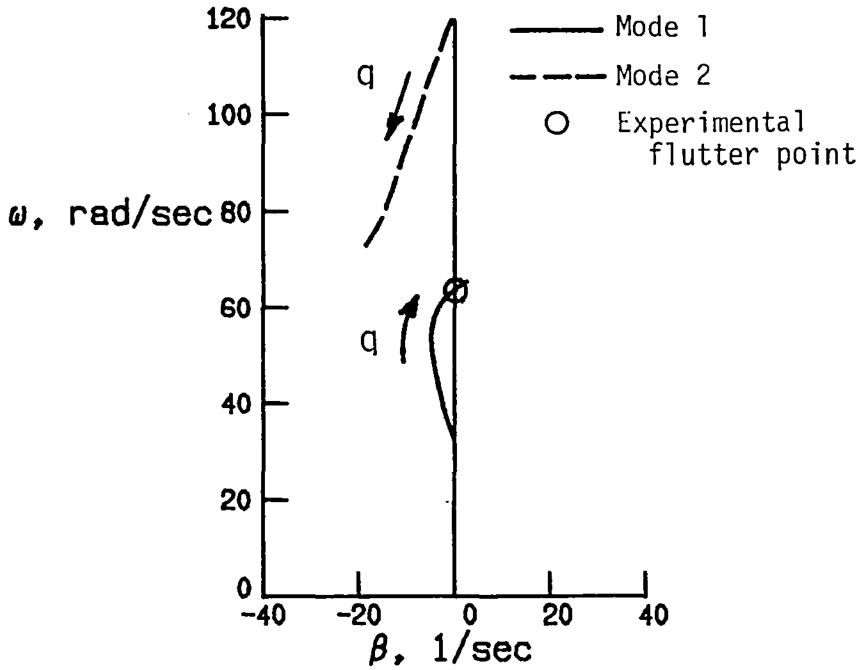

(b) Root locus.

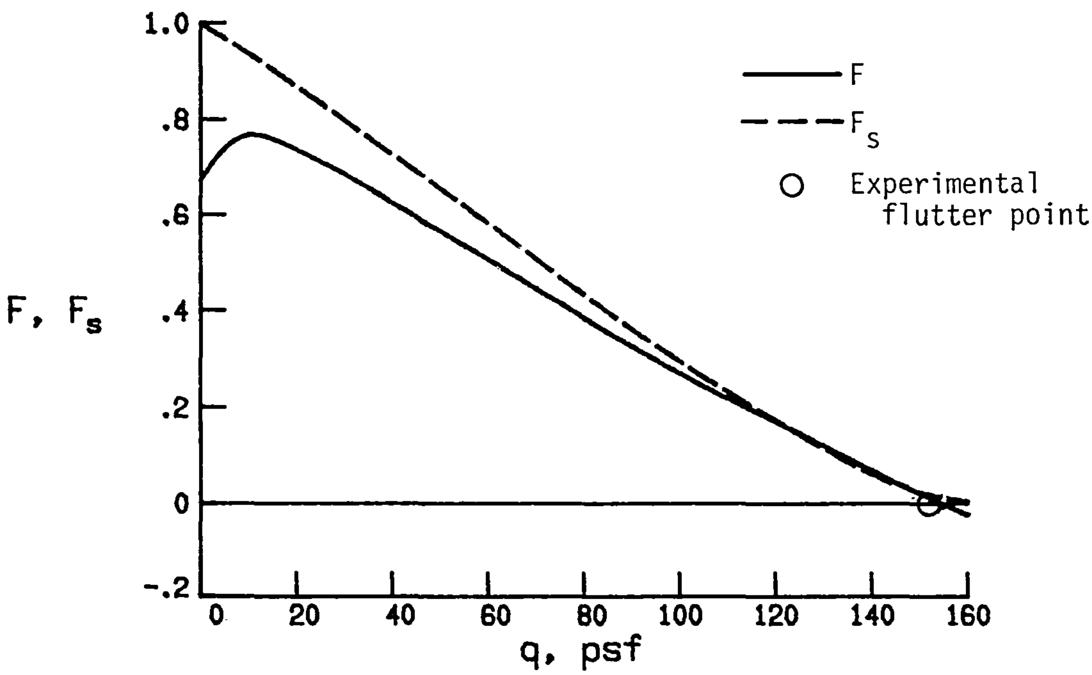

(c) Calculated flutter margin.

Figure 2.- Concluded.

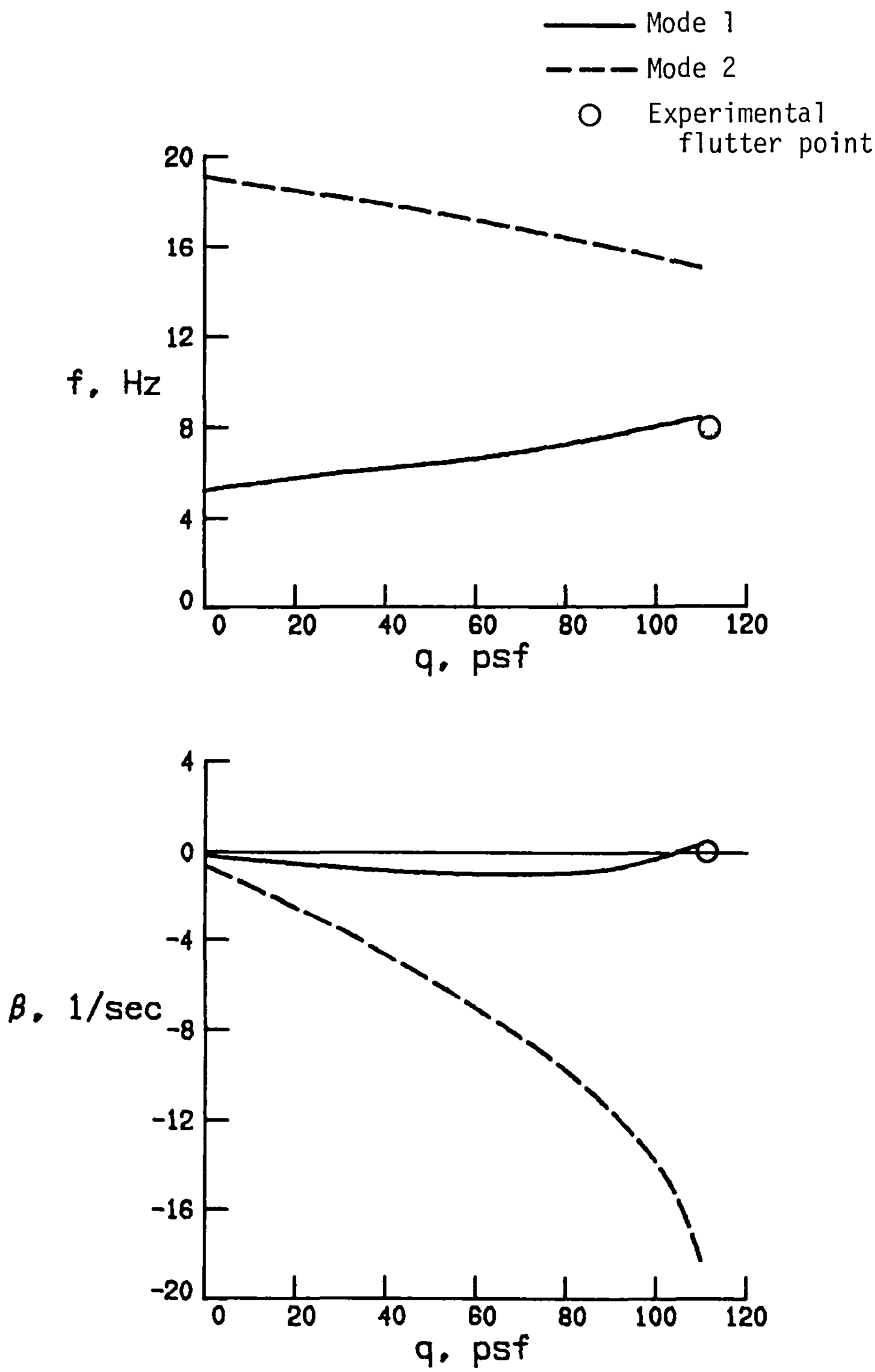

(a) Frequencies and decay rates.

Figure 3.- Calculated dynamic characteristics for wind-tunnel model for $M = 0.9$.

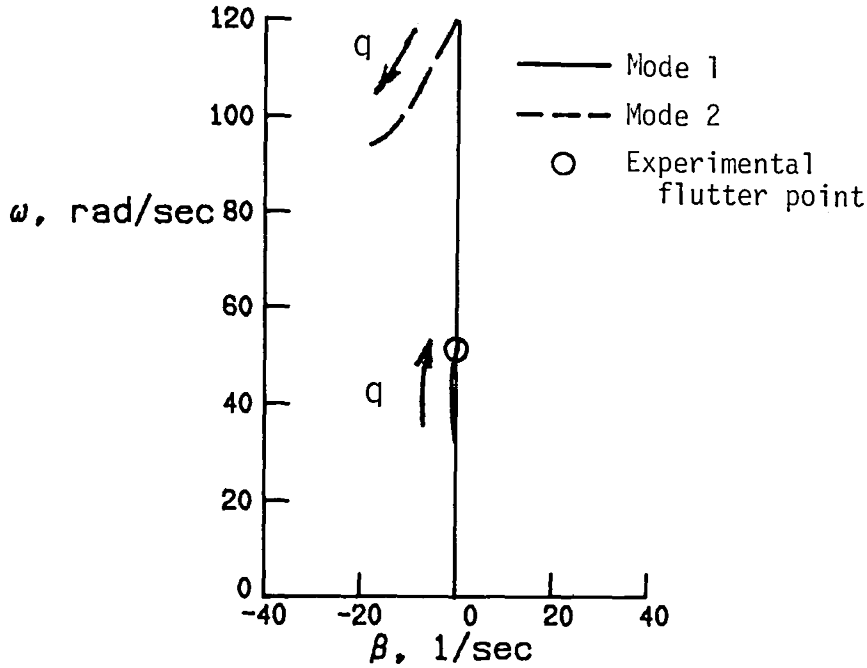

(b) Root locus.

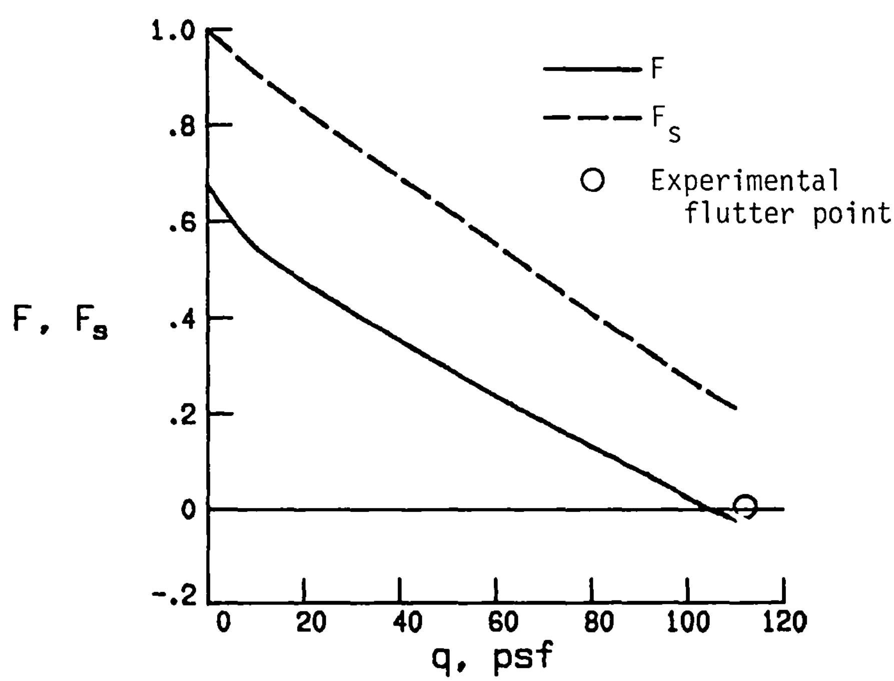

(c) Calculated flutter margin.

Figure 3.- Concluded.

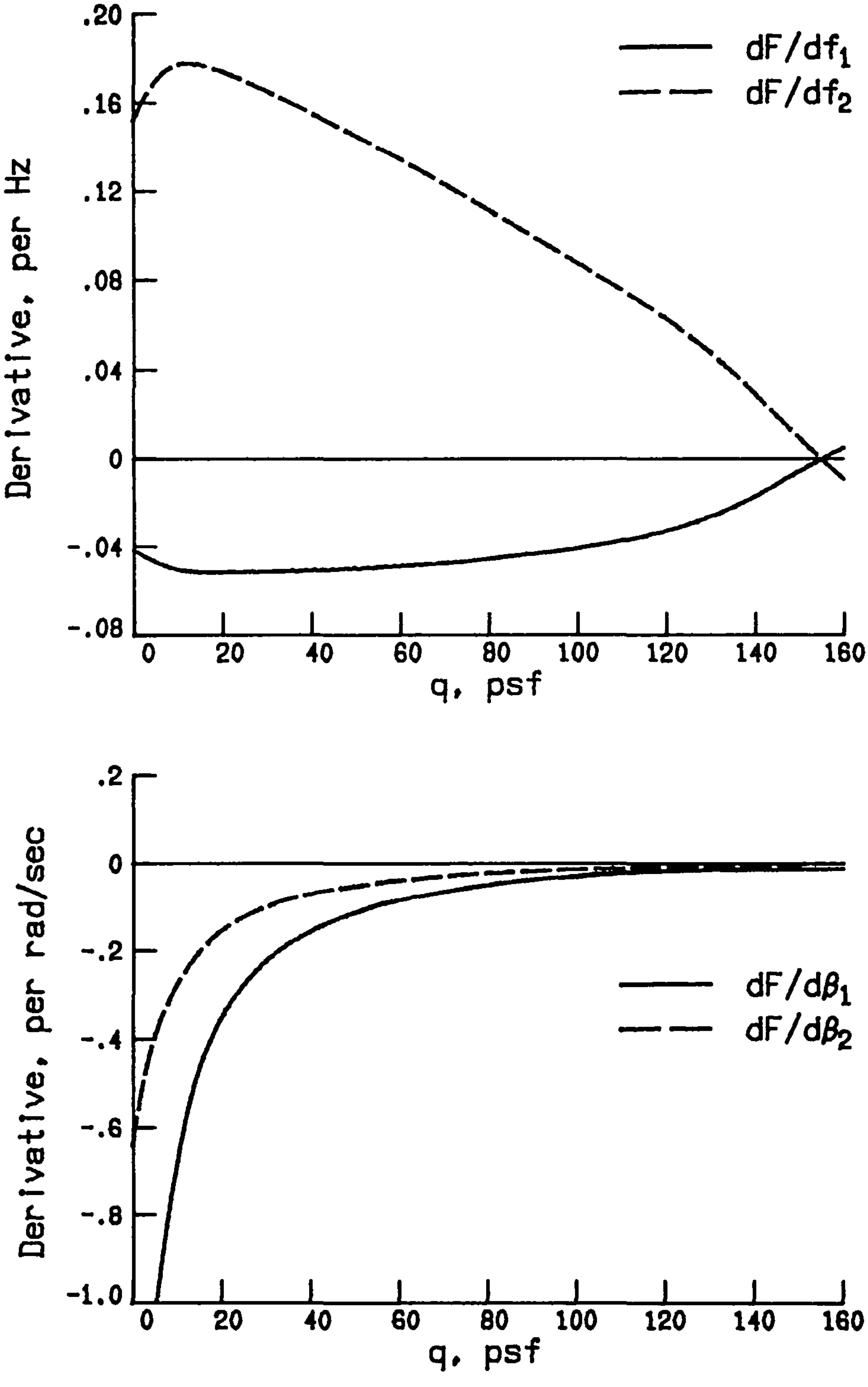

Figure 4.- Calculated derivatives of flutter-margin parameter F for M = 0.6.

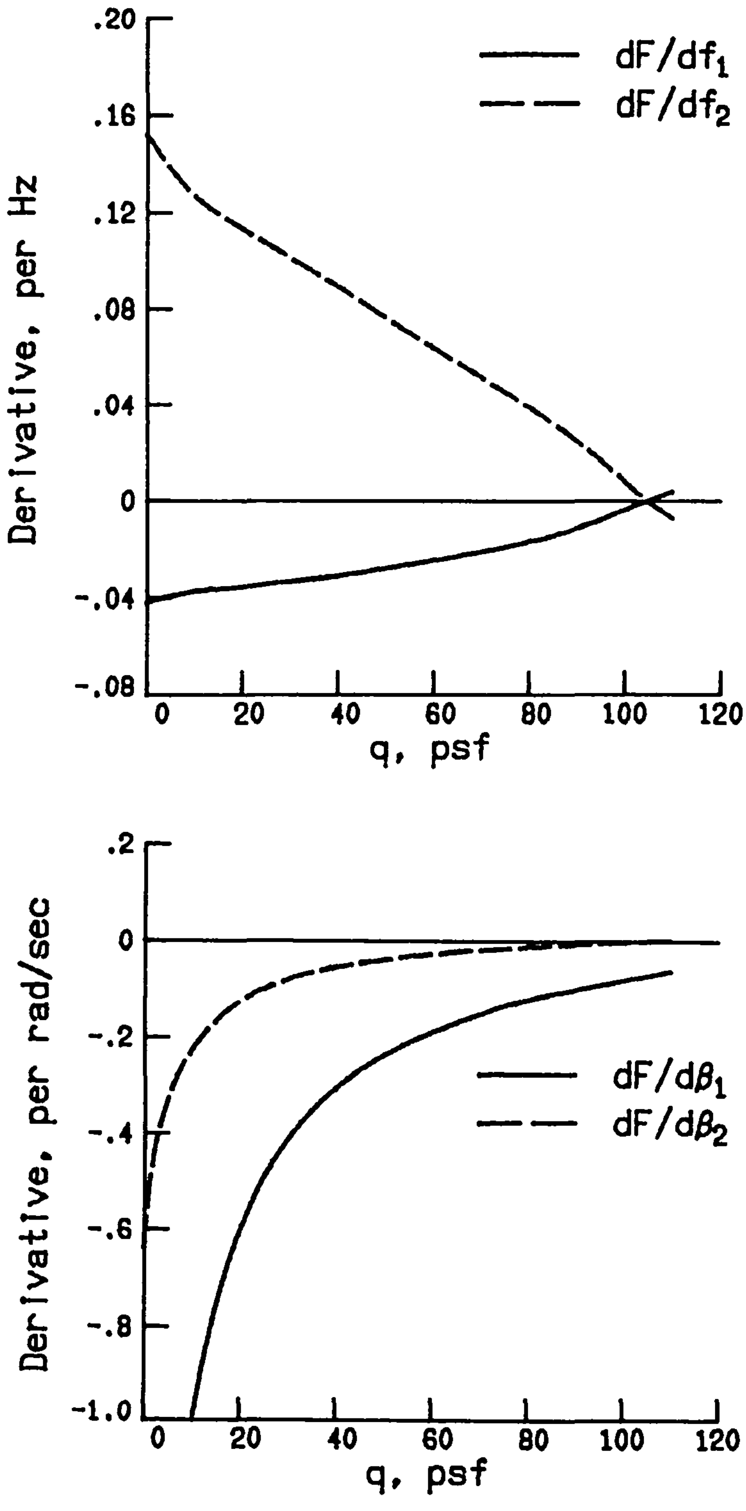

Figure 5.- Calculated derivatives of flutter-margin parameter F for M = 0.9.

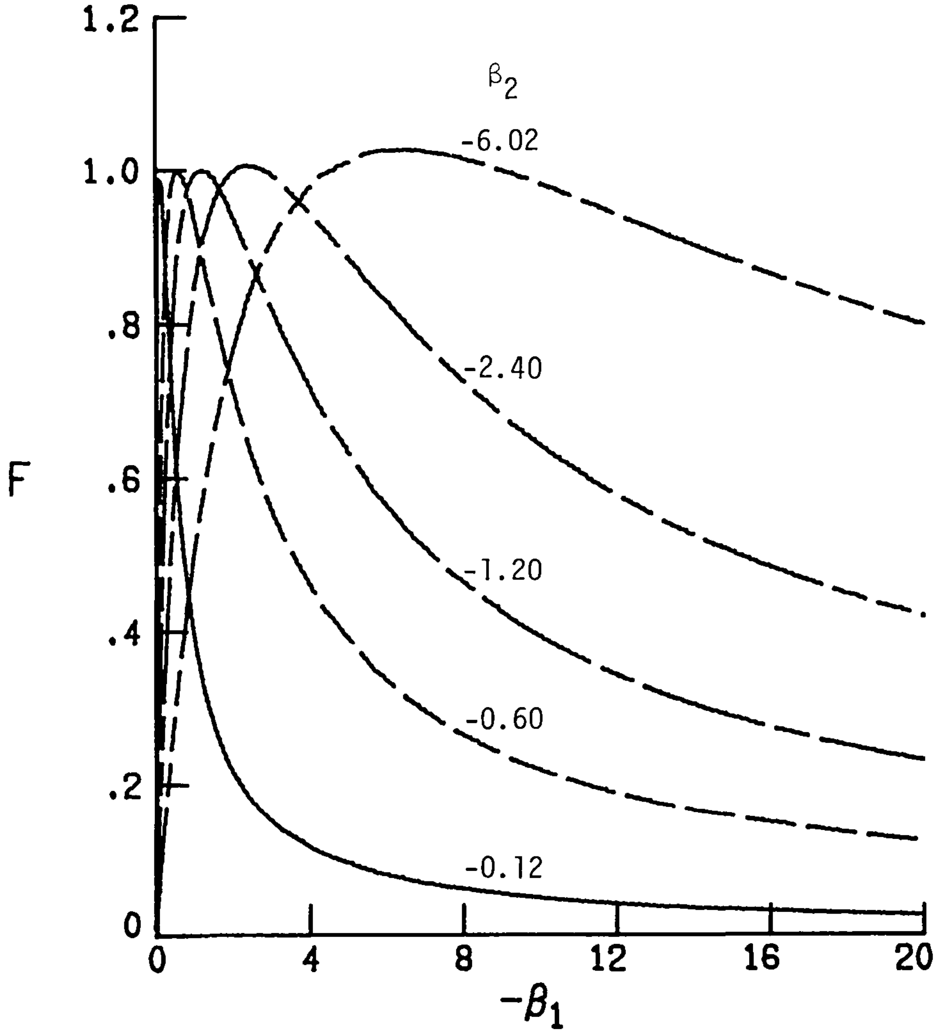

(a) Variation with $-\beta_1$. f_1 = 5.23 Hz; f_2 = 19.13 Hz.

Figure 6.- Variation of F with frequency and damping parameters.

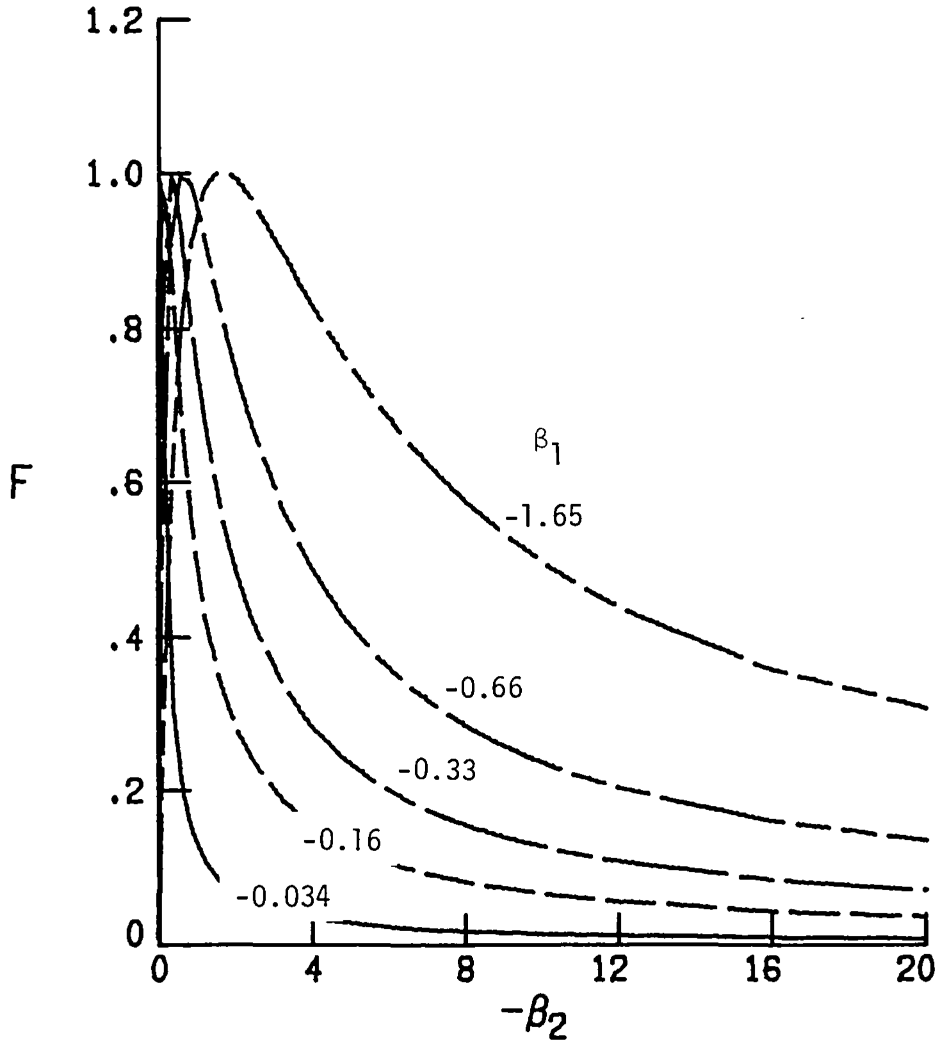

(b) Variation with $-\beta_2$. f_1 = 5.23 Hz; f_2 = 19.13 Hz.

Figure 6.- Continued.

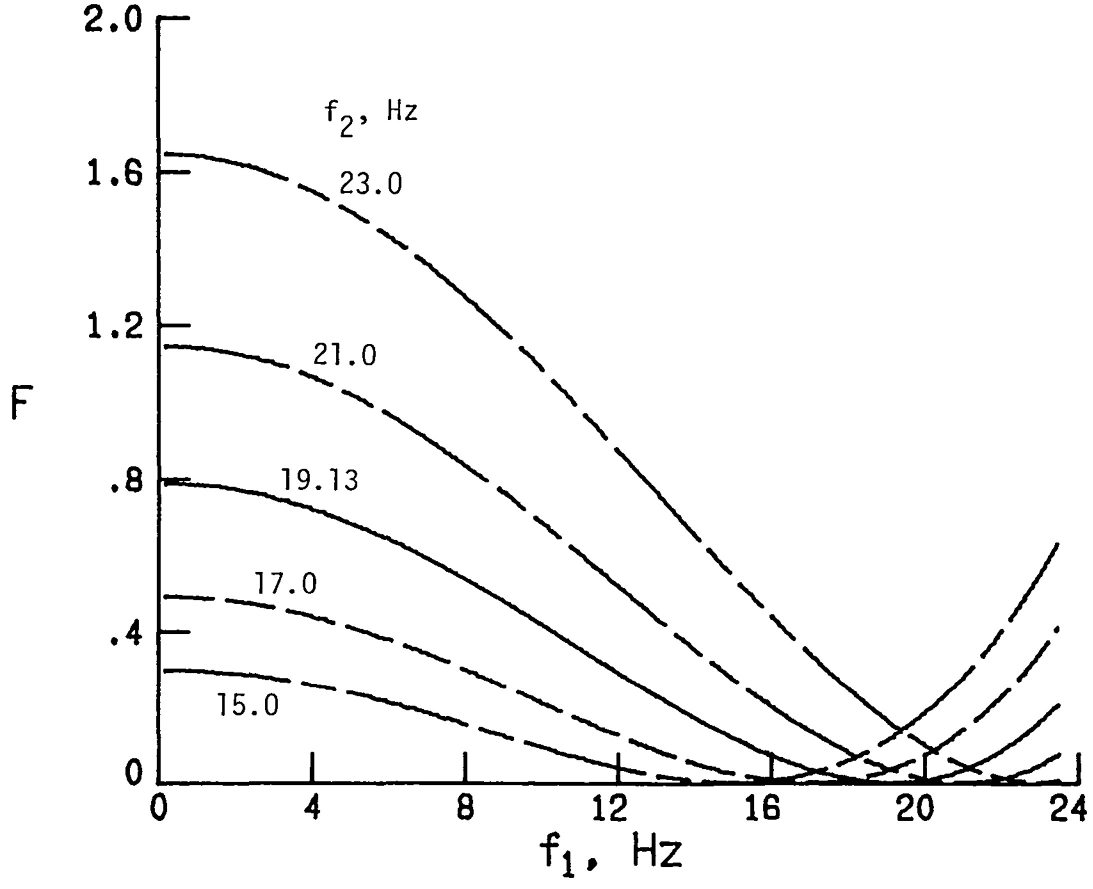

(c) Variation with f_1. $\beta_1 = -0.16$; $\beta_2 = -0.60$.

Figure 6.- Continued.

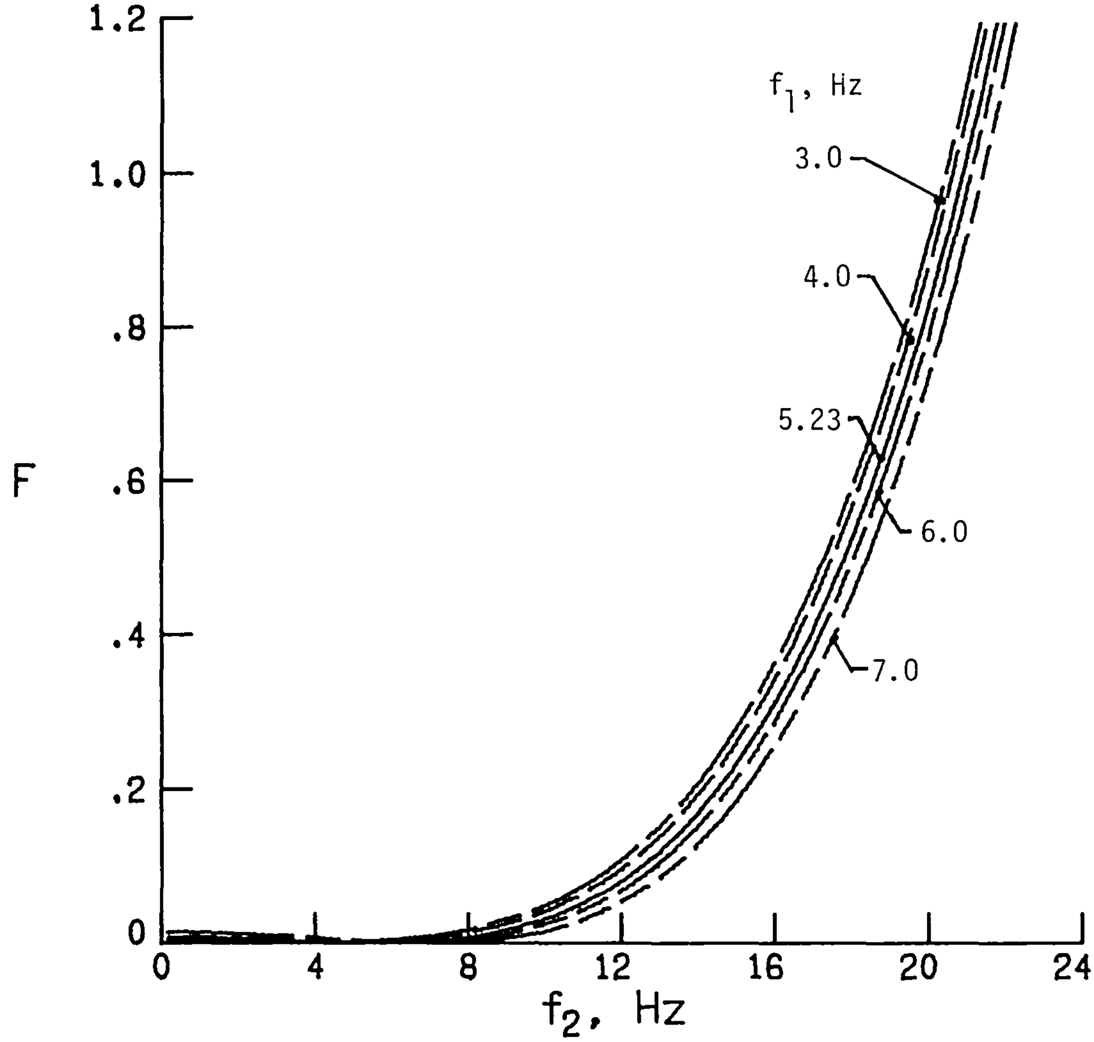

(d) Variation with f_2. $\beta_1 = -0.16$; $\beta_2 = -0.60$.

Figure 6.- Concluded.

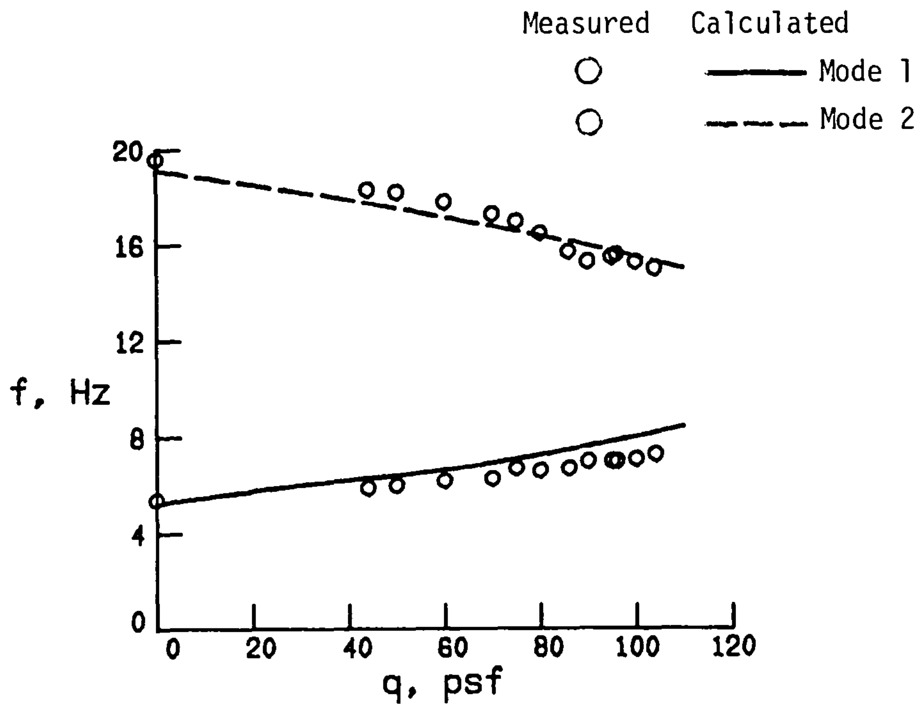

(a) M = 0.9.

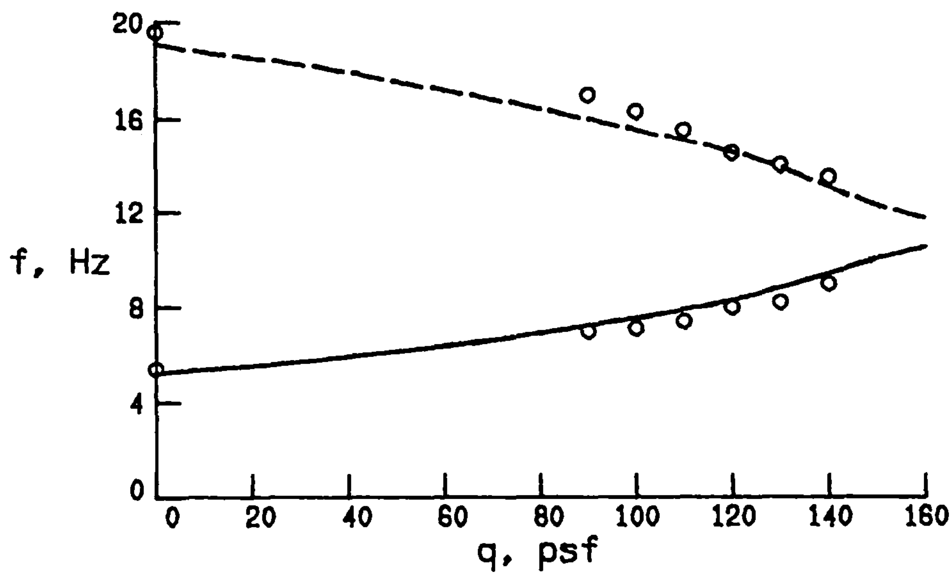

(b) M = 0.6.

Figure 7.- Comparison of calculated frequencies with frequencies determined from power spectral measurements.

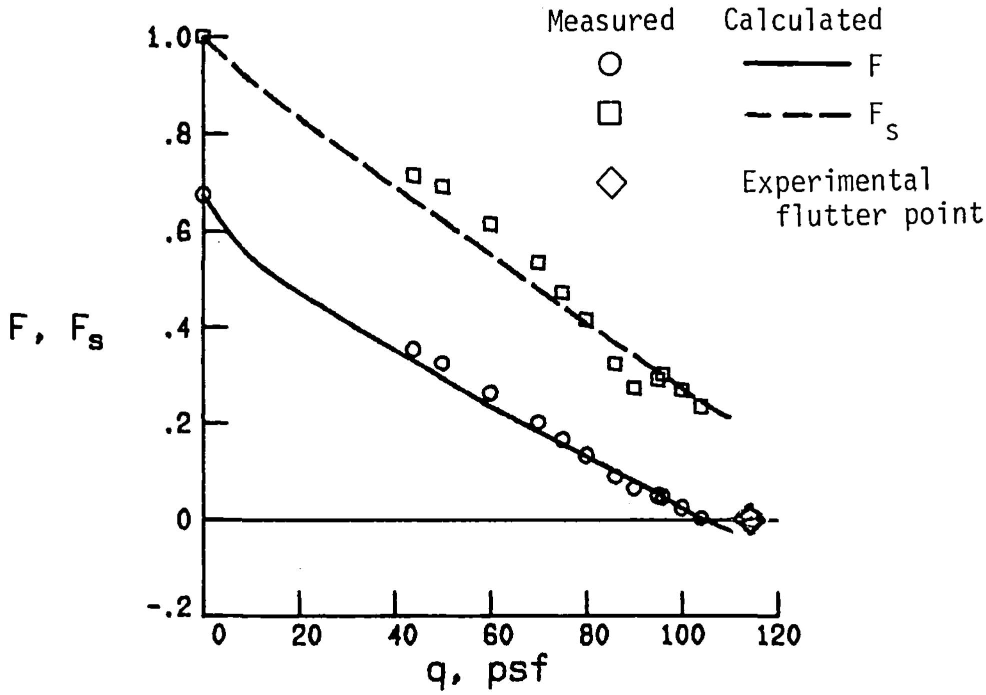

(a) M = 0.9.

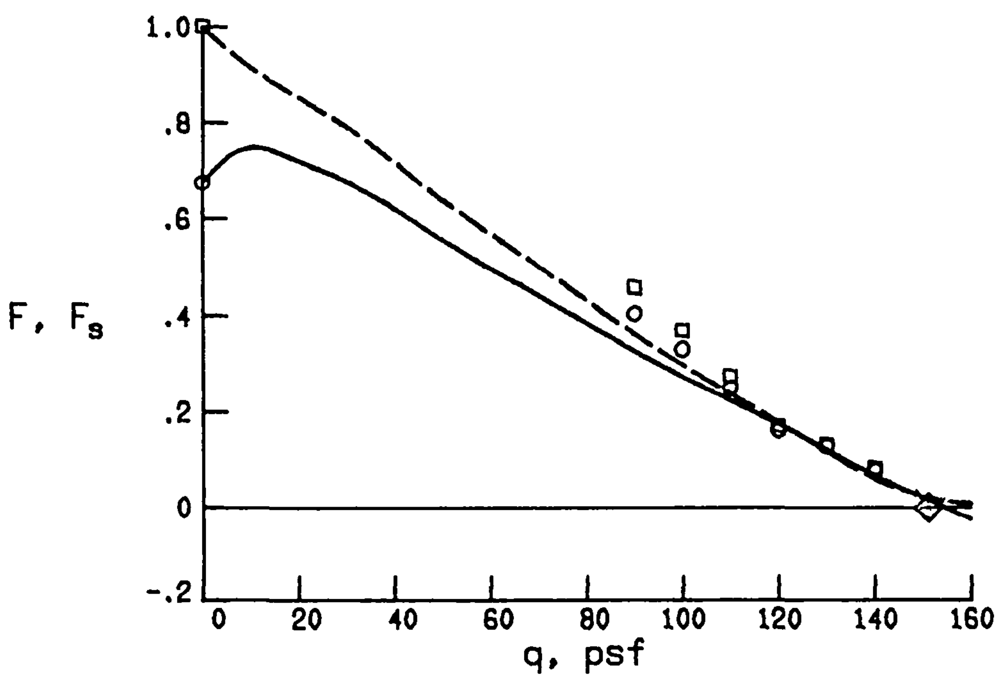

(b) M = 0.6.

Figure 8.- Comparison of flutter-margin parameters by using calculated and measured frequencies.

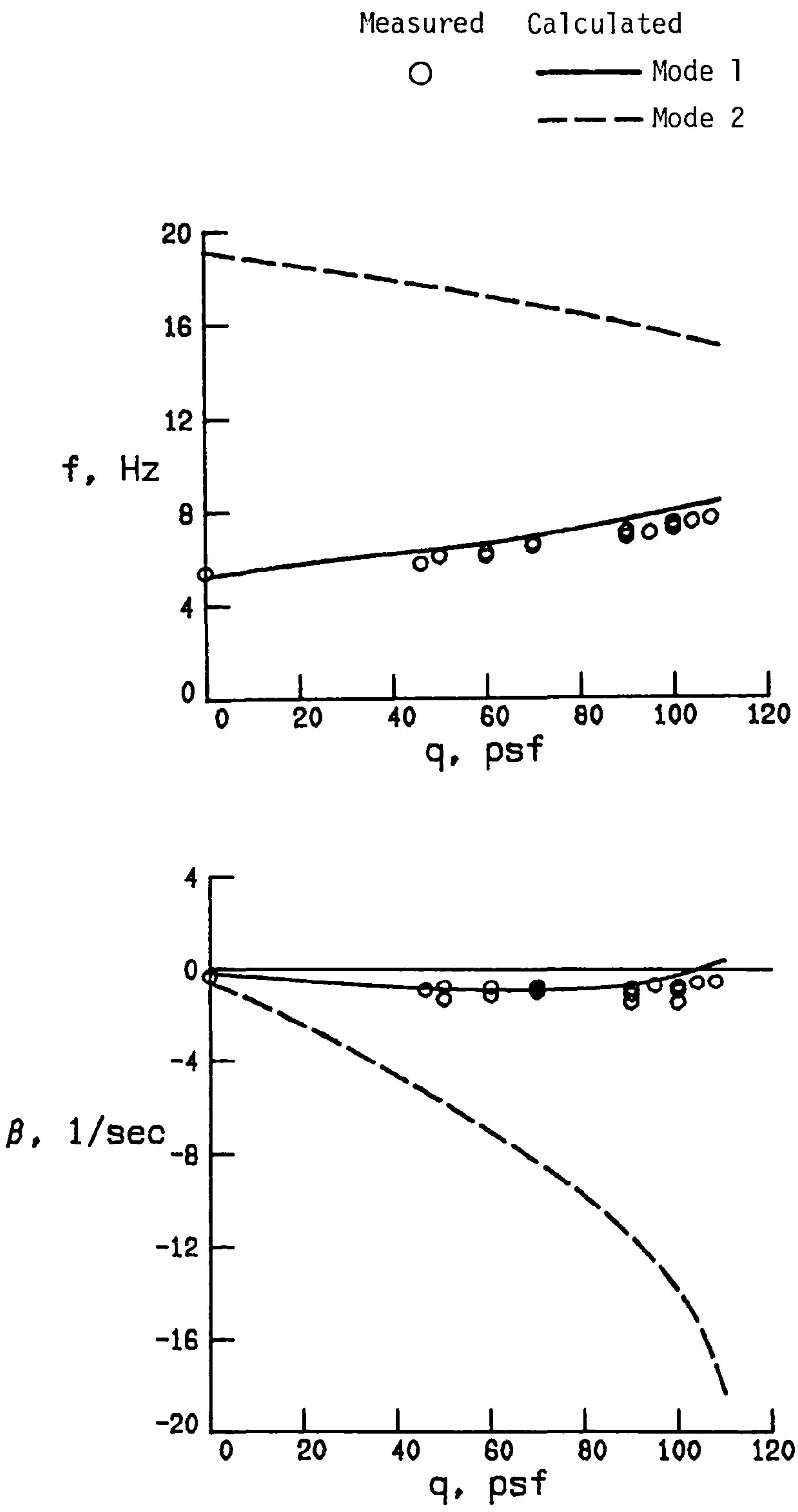

Figure 9.- Comparison of calculated dynamic characteristics with first-mode experimental data from fast frequency sweeps. M = 0.9.

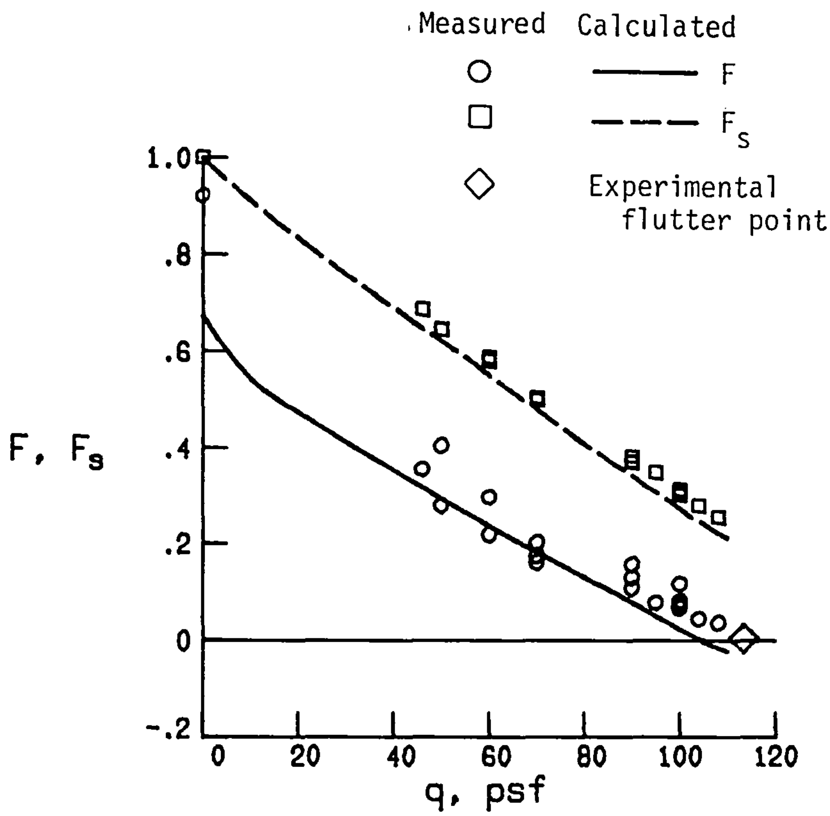

Figure 10.- Comparison of flutter-margin parameters by using calculated and measured first-mode data. M = 0.9.

1. Report No.	2. Government Accession No.	3. Recipient's Catalog No.
NASA TM-84545		

4. Title and Subtitle	5. Report Date
APPLICATION OF ZIMMERMAN FLUTTER-MARGIN CRITERION TO A WIND-TUNNEL MODEL	November 1982
	6. Performing Organization Code 505-33-53-07
7. Author(s) Robert M. Bennett	8. Performing Organization Report No. L-15508
	10. Work Unit No.
9. Performing Organization Name and Address NASA Langley Research Center Hampton, VA 23665	11. Contract or Grant No.
	13. Type of Report and Period Covered Technical Memorandum
12. Sponsoring Agency Name and Address National Aeronautics and Space Administration Washington, DC 20546	14. Sponsoring Agency Code

15. Supplementary Notes

16. Abstract

A brief study of the Zimmerman flutter-margin criterion has been made by applying it to data obtained from a wind-tunnel model. The sensitivity of the flutter-margin parameter was explored with a parametric trend study and by calculation of the derivatives with respect to the input frequency and damping parameters. The criterion is simple in concept and application, and it serves as a good flutter-onset predictor because it gives a nearly linear variation with dynamic pressure. However, accurate values of both frequency and damping of both modes involved in flutter are required for reliable flutter-onset prediction. The simplified version using only frequencies gave a highly nonconservative flutter onset in one case and should not be used in general.

17. Key Words (Suggested by Author(s))	18. Distribution Statement
Flutter Subcritical response Routh's discriminant Zimmerman criterion	Unclassified - Unlimited Subject Category 05

19. Security Classif. (of this report)	20. Security Classif. (of this page)	21. No. of Pages	22. Price
Unclassified	Unclassified	29	A03

National Aeronautics and
Space Administration

Washington, D.C.
20546

Official Business
Penalty for Private Use, $300

THIRD-CLASS BULK RATE

Postage and Fees Paid
National Aeronautics and
Space Administration
NASA-451

U.S.MAIL

NASA

POSTMASTER: If Undeliverable (Section 158 Postal Manual) Do Not Return